Journal of Thermal Analysis and Calorimetry, Vol. 61 (2000) 889–896

ANNEALING AND CRYSTALLIZATION OF $Fe_{40}Ni_{40}P_{14}B_6$ GLASSY ALLOY A DSC study

F. Branda, G. Luciani and A. Costantini

Dipartimento di Ingegneria dei Materiali e della Produzione, Universitŕ di Napoli, P.le Tecchio I-80125 Napoli, Italy

(Received October 19, 1999; in revised form April 17, 2000)

Abstract

In this paper a DSC study is reported of the behavior of $Fe_{40}Ni_{40}P_{14}B_6$ alloy produced by rapid quenching. The experimental results show that relaxation phenomena can be studied directly from the DSC curves. From these experiments, the spread of the E_c values in the literature is attributed to differences in the quenching rates and the presence of variable number of quenched-in nuclei. It is also shown that the microstructure (number and size of crystals) of the non-isothermally devitrified metallic alloy changes with the heating rate; this is a consequence of the shift of crystallization temperatures and, therefore, of the change of the ratio of nucleation and crystal growth rates.

Keywords: crystallization, DSC, $Fe_{40}Ni_{40}P_{14}B_6$ glassy alloy

Introduction

Metallic glasses are widely studied for their very interesting physical and electrical properties. When subjected to thermal treatments their properties can vary strongly as a consequence of either short-range structural changes, due to annealing at relatively low temperatures, or more important modifications, due to nucleation and growth of new phases at higher temperatures.

One of the best known and studied alloys has the composition $Fe_{40}Ni_{40}P_{14}B_6$ (Metglas 2826). Recently [1], it was shown that information on the effect of the annealing could be obtained by studying its effect on thermal expansion. Isothermal and non-isothermal [2–10] studies of the crystallization behavior were published. Crystallization activation energy, E_c, values widely changing in the range 370–490 kJ mol^{-1} were obtained mostly by means of non-isothermal methods. In the case of non-isothermal studies, however, only as quenched samples were examined.

In this paper a DSC study is reported of the behavior of $Fe_{40}Ni_{40}P_{14}B_6$ alloy produced by rapid quenching. In particular, the effect of isothermal and non-isothermal heat treatments on the recorded DSC curve are studied in order to both probe the

1418–2874/2000/ $ 5.00

Akadémiai Kiadó, Budapest
Kluwer Academic Publishers, Dordrecht

non-isothermal devitrification behavior, to find an explanation to the spread of E_c values and evaluate if it is possible to get information on the short range structural changes during annealing.

Experimental

The amorphous ribbons, ~16 μm thick, used for this investigation were prepared by means of the single roller technique of rapid quenching from the melt; the average tangential velocity of the roller on which the melt was ejected was 35 m s^{-1}, they were produced in the Italian National Electrotechnic Institute 'G. Ferraris'. The samples for the different heat treatments were all cut from the same ribbon.

Differential Thermal Analysis (DTA) was carried out by means of a Netzsch Differential Scanning Calorimeter (DSC) heat flux model 404M on about 5 or 40 mg samples at various heating rates (2–80°C min^{-1}) in an inert atmosphere (helium). Powdered Al_2O_3 was used as reference material.

Isothermal heating was carried out in a furnace with a fine control of the temperature; when the planned temperature was reached and stabilized, a little cell, containing the sample, was inserted into the furnace. Static helium atmosphere was maintained in the cell during the treatment. When the prefixed time was elapsed, the cell was taken out from the furnace and the sample was cooled, in about 2 min, to room temperature in a stream of helium.

Results

Figure 1 shows the typical behaviour of two cases obtained with several samples of $Fe_{40}Ni_{40}P_{14}B_6$. In the case of Fig. 1a, just after the slope change in the glass transformation range an exothermic peak of crystallization appears. As usual, the exo-peak is shifted when the heating rate, β, is changed: the onset, T_o, and peak, T_p, temperatures change from T_o=414 and T_p=422°C for β=20°C min^{-1}, to T_o=397 and T_p=408°C for β=2°C min^{-1}. Several samples were variously heat treated without any effect on the exo-peak recorded at 20°C min^{-1}: 1 h at T=300, 350 and 380°C and a thermal treatment in DSC apparatus at β=2°C min^{-1} till the onset of the crystallization exo-peak. Some changes in the DSC curve were recorded when the non-isothermal treatment at β=2°C min^{-1} was prolonged to T=401°C: the crystallization peak, appearing on the curve recorded in the subsequent run at β=20°C min^{-1} (Fig. 1b) becomes broader and is so shifted towards lower temperatures as to hide the slope change at the glass transition temperature, T_g. In Fig. 2 the same curves, but the 1b one, are reported in an expanded scale. As can be seen a slope change of the baseline occurs at about 200°C. All the annealed samples show greater slope change at 200°C than the as-quenched one. All the curves were recorded working with a particularly large mass of sample (40 mg) in the same experimental conditions (same heating rate, same mass of the sample, etc.). Therefore, the differences in the slope changes from one curve to another must be ascribed to differences, induced by thermal treatments, in the depend-

ence of the specific heat coefficient, c_p, on the temperature. Figure 2b shows, however, a singular behavior: the slope change at T=200°C is followed by a second reverse one at T=340°C.

The non-isothermal devitrification is well described by the well known following equation [11, 12]:

$$-\ln(1-\alpha)=(AN/\beta^m)\exp(-mE_c/RT) \quad (1)$$

where α is the crystallization degree, N the nuclei number per unit volume, A is a constant, β the heating rate, E_c the crystallization activation energy and m a parameter that depends on the crystallization mechanism.

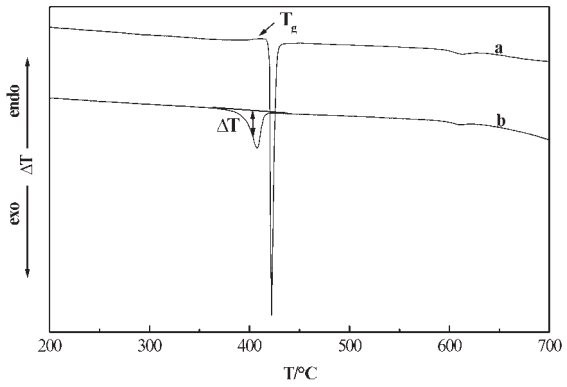

Fig. 1 DSC curves at β=20°C min^{-1} for the $Fe_{40}Ni_{40}P_{14}B_6$ metallic glass. a – as-quenched, 1 h at T=300°C, 1 h at T=350°C, 1 h at T=380°C, 2°C min^{-1} to T=396°C, b – 2°C min^{-1} to T=401°C

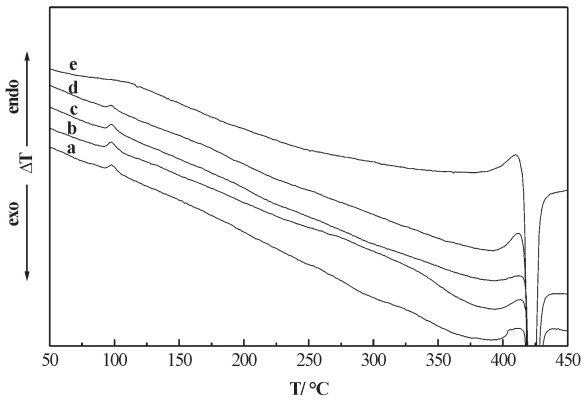

Fig. 2 DSC traces at β=20°C min^{-1}, till T_g, before (a curve) and after annealing m (other curves). a – as-quenched, b – 1 h at T=300°C, c – 1 h at T=350°C, d – 1 h at T=380°C, e – after DSC 2°C min^{-1} to T=396°C

If the value of α at the peak temperature, T_p, is not dependent on the heating rate [13] Eq. (1) gives:

$$\ln\beta = -E_c/RT_p + const. \quad (2)$$

If the deflection from the baseline, ΔT, is proportional to the instantaneous reaction rate [14, 15] and, in the initial part of the DTA crystallization peak, the change in the temperature has a much greater effect than α on ΔT [16] Eq. (1) also gives:

$$\ln\Delta T = -mE_c/RT + const. \quad (3)$$

It's worth reminding that Eqs (2) and (3) can also be derived [17] by considering that the crystallization is well described by the well known Johnson-Mehl-Avrami equation, that the deflection from the baseline is proportional to the instantaneous reaction rate and that, at T_p, $d(\Delta T)/dT = d(d\alpha/dt)/dT = 0$.

It's also worth pointing out that the crystallization activation energy, E_c, reduces to the crystal growth activation energy when the sample is well nucleated in a previous heat treatment before DTA.

The results for the several samples variously heat-treated are resumed in Table 1. In Fig. 3 the plots of $\ln\beta$ *vs.* $1/T_p$ are reported for the as quenched and the (g) sample of Table 1; in Fig. 4 the plots of $\ln\Delta T$ *vs.* $1/T$ are reported. According to Eqs (2) and (3), straight lines were obtained. The values of E_c and mE_c calculated from their slopes are reported in Table 1. As can be seen the non-isothermal heat treatment till 401°C, makes E_c decrease, in addition to the shift of the peak in the subsequent run at 20°C min^{-1} (Fig. 1b). As shown in Table 1, in the case of samples a–d, a constant value mE_c=3200±250 kJ mol^{-1} was found. The mE_c value is, instead, influenced by the non-isothermal treatments, at 2°C min^{-1}, stopped at higher temperatures than the crystallization exo-peak onset (T=397°C). The higher the final temperature of these treatments is, the lower mE_c is.

Table 1 Peak temperatures, crystallization activation energies, E_c, and product of the Avrami parameter and crystallization activation energy, mE_c, of the variously heat treated $Fe_{40}Ni_{40}P_{14}B_6$ samples

Sample	Thermal treatment	T_p/°C	E_c/kJ mol^{-1}	mE_c/kJ mol^{-1}
a	as quenched	421.6	485	3110
b	1h 300°C	421.6		3450
c	1h 380°C	421.6		2960
d	2°C min^{-1} till 396°C	420.3		3110
e	2°C min^{-1} till 399°C	419.5		1870
f	2°C min^{-1} till 400°C	417.0		1298
g	2°C min^{-1} till 401°C	407.6	360	536
h	2°C min^{-1} till 403°C	408.7		450

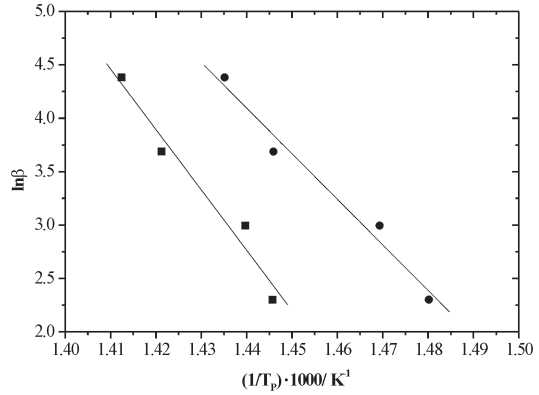

Fig. 3 Plot of lnβ *vs.* $1/T_p$. ■ – as-quenched, ● – 2°C min^{-1} to *T*=401°C

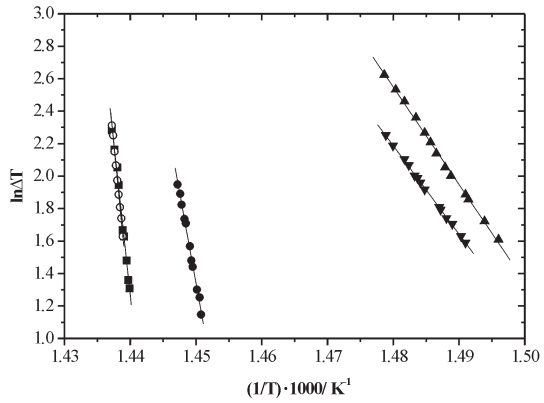

Fig. 4 Plot of lnΔ*T* *vs.* 1/*T*. ■ – as-quenched, o – 1 h at *T*=300°C, ● – 2°C min^{-1} to *T*=399°C, ▲ – 2°C min^{-1} to *T*=401°C, ▼ – 2°C min^{-1} to *T*=403°C

Discussion

Figure 2 shows that the structural relaxation occurring during the annealing causes detectable changes of the DSC baseline linked to differences in the dependence of c_p on the temperature. It's known that structural relaxation can give rise to topological short range ordering (TSRO) and compositional short range ordering (CSRO) [18–20]. In TSRO relaxation causes only slight distortion of polyhedral structural units and changes their stacking configurations. In this way, a redistribution and transformation of the quenched in structural defects takes place. CSRO, instead, involves exchange of atoms of different chemical species. All this can well justify the above-observed changes of c_p after the annealing. One explanation for the singular shape of the 2b curve can be given by the known crossover effect [21]. As it is known,

the variation of some glasses properties, such as the refractive index or the Curie temperature of metallic glasses, with time and temperature of annealing, were explained by admitting two relaxation mechanisms having very different relaxation times [21]. If we admit that this happens also in the case of $Fe_{40}Ni_{40}P_{14}B_6$ alloy and that the faster mechanism is dominant at a lower temperature (300°C) while the slower one at a higher temperature (350–380°C), an explanation to the 2b curve can be found. In fact, when the sample taken 1 h at 300°C is heated in the DSC apparatus, a rapid regression of the faster relaxation mechanism should take place above 300°C, while the other one should slowly occur. As a consequence, the first slope change would be followed by a second reverse one. The two mechanisms could well be, as already supposed for other alloys [21], TSRO and CSRO.

When nucleation occurs in a glass, usually the peak temperature and shape of the crystallization peak, during a subsequent DTA run, are strongly influenced [22]: the greater the nuclei number is, the more the peak shifts towards lower temperatures and the sharper it becomes.

The experimental results reported in Table 1 show that the exo-peak temperature and shape (that according to Eq. (3) is related to mE_c value) and the estimated values of the crystallization activation energy, E_c, are strongly influenced only by the non-isothermal pre-treatments at β=2°C min^{-1} stopped at temperatures higher than the crystallization onset. In particular, E_c decreases, when the alloy is preheated at 2°C min^{-1} till 401°C (sample g in Table 1), from the value E_c=485 to E_c=360 kJ mol^{-1}. It's interesting to observe that the values reported in the literature for the overall crystallization activation energy, all referring to as quenched alloys, differ considerably from one another: E_c=440 kJ mol^{-1} [6], E_c=385 kJ mol^{-1} [2], E_c=430 kJ mol^{-1} [3], E_c=367 kJ mol^{-1} [5]. All of them fall between the two values found in this work. All this is well explained if we consider that usually, in the case of metallic glasses, the curves of nucleation and crystal growth rates are well superimposed. In this case the nuclei number formed in the course of the crystallization process can be not negligible with respect to the one already formed at the onset temperature of crystallization, T_0; it was proposed [6] that in this case E_c is related to the nucleation, E_n, and crystal growth, E_g, activation energies by the following relation [6]:

$$E_c=(aE_n+bE_g)/(a+b) \quad (4)$$

where a=0 for nucleation rate zero, a=1 for constant nucleation rate; b depends on the mechanism and morphology of crystal growth; it ranges from b=1 for 1-dimensional growth (or growth from surface nuclei) to b=3 for 3-dimensional growth [6, 11, 12] if the process is controlled by the reaction at the interface; it ranges from b=1/2 for 1-dimensional growth (or growth from surface nuclei) to b=1.5 for 3-dimensional growth [6, 11, 12] if the process is diffusion controlled; m is the Avrami parameter; in particular $m=a+b$ [6].

Obviously, the ratio of the nucleation and crystal growth rates varies with temperature. As a consequence the number and size of the formed crystals should depend on the heating rate. In fact, when β is increased the crystallization peak is shifted towards higher temperatures, where the ratio of the nucleation and crystal growth rates

is different. If this ratio decreases when the temperature is increased, the lower the heating rate is, the finer the microstructure should be, that is the greater the number and the smaller the size of the formed crystals. As a consequence, when crystallization during a run at lower β (2°C min^{-1}) is stopped before completion, the sample is cooled to room temperature and thereafter reheated at higher heating rate (20°C min^{-1}), the crystallization peak is expected to occur at lower temperature than in the absence of pre-treatment, owing to the greater number of nuclei that grow. Therefore, the shift of the peak of sample (g) with respect to sample (a) is well explained. Moreover, the peak shift is so great that, taking into account previous works [22, 23], we can expect that the new nuclei formed during the second run at 20°C min^{-1} are negligible with respect to those already formed during the first run at 2°C min^{-1}. If this is true, in the case of sample (g), according to Eq. (4), it is expected that $E_c=E_g$ while, in the case of sample (a), it should be an average value between E_n and E_g. This is confirmed by the values of the activation energy for nucleation, E_n=740 and crystal growth, E_g=345 kJ mol^{-1} determined by quantitative transmission electron microscopy (TEM), that is by counting the nuclei and measuring crystal sizes, that are reported in literature [4, 6]. In fact, the second value (E_g) is very close to E_c=360 kJ mol^{-1} relative to the 'nucleated' (g) sample. Taking the particularly high value of E_n into account, according to Eq. (4), the greater observed value of E_c of sample (a) is also justified. The reminded differences among the literature values can also be explained: they could simply imply that the studied glasses had different thermal histories, which could simply be the result of different quenching rates and the presence of a variable number of quenched-in nuclei. It's interesting to observe that it has been recently reported [10], on the basis of optical observation, that in the case of $Fe_{40}Ni_{40}P_{14}B_6$ the average grain size increases while the crystal number decreases when the heating rate is increased.

The mE_c values reported in Table 1 appear not to be influenced by the thermal treatments b–d; a variation is observed when non-isothermal preheating at 2°C min^{-1} is stopped after the crystallization onset temperature. The value for samples a–d, $m\approx6$ is higher than the $m\approx4$ previously found [2, 3, 6]. However, recently, a similar value of m was found [10] that was linked to non-steady state nucleation. It is interesting to observe that, as can be deduced from Table 1, it reduces however progressively as a function of the thermal pre-treatment till $m\approx1$ (sample h). This decrease cannot be simply explained by the reduction to zero of the parameter a in the above reported relation $m=a+b$. The results suggest that, as a consequence of the thermal treatment, the mechanism of crystal growth also changes.

Conclusions

The experimental results suggest that

1. relaxation phenomena can be studied directly from DSC curves;
2. the spread of E_c values found in the literature, can be attributed to differences in the quenching rates and the presence of variable number of quenched-in nuclei;

3. the microstructure (number and size of crystals) of the non-isothermally devitrified metallic alloy changes with the heating rate; this is the consequence of the shift of the crystallization peak and of the consequent change of the ratio of nucleation and crystal growth rates.

* * *

The work was supported by the National Institute for Matter Physics (INFM) as part of the project for 'Magnetoelastic sensors production for the measure of displacements, vibrations and mass flows'.

References

1 J. Steinberg, S. Tyagi and A. E. Lord Jr., J. Non-Cryst. Solids, 41 (1980) 279.
2 M. G. Scott, J. Mat. Sci., 13 (1978) 291.
3 T. Watanabe and M. Scott, J. Mat. Sci., 15 (1980) 1131.
4 D. G. Morris, Acta Met., 29 (1981) 1213.
5 C. Antonione, L. Battezzati, A. Lucci, G. Riontino and G. Venturello, Scripta Met., 12 (1978) 1011.
6 S. Ranganathan, M. Von Heimendahl, J. Mat. Sci., 16 (1981) 2401.
7 D. G. Morris, Scripta Metall., 16 (1982) 585.
8 Y. Limoge and A. Barbu, Acta Metall., 30 (1982) 2233.
9 R. S. Tiwari, J. Non-Cryst. Solids, 83 (1986) 126.
10 V. I. Tkatch, A. I. Limanovskii and V. Yu. Kameneva, J. Mat. Sci., 32 (1997) 5669.
11 K. Matusita and S. Sakka, Bull. Inst. Chem. Res., Kyoto Univ., 59 (1981) 159.
12 D. R. MacFarlane, M. Matecki and M. Poulain, J. Non-Cryst. Solids, 64 (1984) 351.
13 P. G. Boswell, J. Thermal Anal., 18 (1980) 353.
14 H. J. Borchardt and F. Daniels, J. Am. Chem. Soc., 79 (1957) 41.
15 K. Akita and M. Kase, J. Phys. Chem., 72 (1968) 906.
16 F. O. Piloyan, I. V. Ryabchica and O. S. Novikova, Nature, 212 (1966) 1229.
17 A. Marotta and A. Buri, Thermochim. Acta, 25 (1978) 155.
18 P. H. Gaskell, J. Non-Cryst. Solids, 32 (1979) 207.
19 H. Hermann and W. Kreher, J. Phys. F: Met. Phys., 18 (1988) 641.
20 Z. G. Liu, X. J. Wu, Y. Chen, X. Wu and X. Y. Qin, J. Non-Cryst. Solids, 109 (1989) 262.
21 A. L. Greer and J. A. Leake, J. Non-Cryst. Solids, 33 (1979) 291.
22 A. Marotta, A. Buri and F. Branda, Thermochim. Acta, 40 (1980) 397.
23 A. Marotta, A. Buri, F. Branda and S. Saiello, Thermochim. Acta, 85 (1985) 231.